10

An Incremental Fuzzy Algorithm for The Balance of Humanoid Robots

Erik Cuevas[1,2], Daniel Zaldivar[1,2], Ernesto Tapia[2] and Raul Rojas[2]
[1]Universidad de Guadalajara, CUCEI, [2]Freie Universität Berlin, Institut für Informatik
Mexico, Germany

1. Introduction

Humanoid robots base their appearance on the human body (Goddard et al., 1992; Kanehira et al., 2002; Konno et al., 2000). Minimalist constructions have at least a torso with a head, arms or legs, while more elaborated ones include devices that assemble, for example, human face parts, such as eyes, mouth, and nose, or even include materials similar to skin. Humanoid robots are systems with a very high complexity, because they aim to look like humans and to behave as they do.

Mechanical control, sensing, and adaptive behaviour are the constituting *logical parts* of the robot that allow it to "behave" like a human being. Normally, researchers study these components by modelling only a *mechanical part* of the humanoid robot. For example, artificial intelligence and cognitive science researches consider the robot from the waist up, because its visual sensing is located in its head, and its behavior with gestures normally uses its face or arms. Some engineers are mostly interested in the autonomy of the robot and consider it from the waist down. They develop mathematical models that control the balance of the robot and the movement of its legs (Miller, 1994; Yamaguchi et al., 1999; Taga et al., 1991), allowing the robot to walk, one of the fundamental behaviours that characterizes human beings.

Examples of such mathematical models are *static* and *dynamic walking*. The static walking model controls the robot to maintain its *center of gravity* (*COG*) inside a stable support region, while the dynamic walking model maintains the *zero moment point* (*ZMP*) inside the support region. Kajita et al. (1992) designed and developed an almost ideal 2-D model of a biped robot. He supposed, for simplicity, that the robot's COG moves horizontally and he developed a control law for initiation, continuation and termination of the walking process. Zhen and Shen (1990) proposed a scheme to enable robot climbing on inclined surfaces. Force sensors placed in the robot's feet detect transitions of the terrain type, and motor movements correspondingly compensate the inclination of robot.

The models mentioned above can be, however, computationally very expensive, and prohibitive for its implementation in microcontrollers. Control algorithms for a stable walking must be sufficiently robust and smooth, to accomplish a balance correction without putting in risk the mechanical stability of the robot. This could be resolved by using a controller that modifies its parameters according to a

Source: Humanoid Robots, New Developments, Book edited by: Armando Carlos de Pina Filho
ISBN 978-3-902613-02-8, pp.582, I-Tech, Vienna, Austria, June 2007

mathematical model, which considers certain performance degree required to offer the enough smoothness.

Fuzzy Logic is especially advantageous for problems which cannot be easily represented by a fully mathematical model, because the process is mathematically too complex and computationally expensive, or some data is either unavailable or incomplete. The real-world language used in Fuzzy Control also enables the incorporation of approximate human logic into computers. It allows, for example, partial truths or multi-value truths within the model. Using linguistic modeling, as opposed to mathematical modeling, greatly simplifies system design and modification. It generally leads to quicker development cycles, easy programming, and fairly accurate control. It is important, however, to underline that fuzzy logic solutions are usually not aimed at achieving the computational precision of traditional techniques, but aims at finding acceptable solutions in shorter time.

The Incremental Fuzzy Control algorithm fulfils the robustness and smoothness requirements mentioned above, even its implementation in microcontrollers. Such an algorithm is relatively simple and computationally more efficient than other adaptive control algorithms, because it consists of only four fuzzy rules. The algorithm demonstrates a smooth balance control response between the walking algorithm and the lateral plane control: one adaptive gain varies incrementally depending on the required performance degree.

The objective of this chapter is to describe the incremental fuzzy algorithm, used to control the balance of lateral plane movements of humanoid robots. This fuzzy control algorithm is computationally economic and allows a condensed implementation. The algorithm was implemented in a PICF873 microcontroller. We begin on the next section with the analysis of the balance problem, and follow later with the description of the controller structure. Afterwards, we explain important considerations about the modification of its parameters. Finally, we present experimental results of algorithm, used on a real humanoid robot, “Dany walker”, developed at the Institut für Informatik of the Freie Universität Berlin.

2. Robot Structure

The humanoid robot “Dany Walker” used in our research was built only from the waist down. It consists of 10 low-density aluminium links. They are rotational on the pitch axis at the hip, knee and ankle. Each link consists of a modular structure. The links form a biped robot with 10 degrees of freedom, see Fig. 1.

The robot structure and its mass distribution affect directly the dynamic of the humanoid (Cuevas et al., 2004), therefore, the movement of the *Center of Masses* (*COM*) has a significant influence on the robot stability. In order to achieve *static* stability, we placed the COM as low as possible. To such purpose, our design uses short legs, see Fig. 2

To compensate the disturbances during walking, our construction enables lateral movements of the robot. Thus, it was possible to control the lateral balance of the robot by swaying the waist using four motors in the lateral plane: two at the waist and two at the ankles, see Fig. 3.

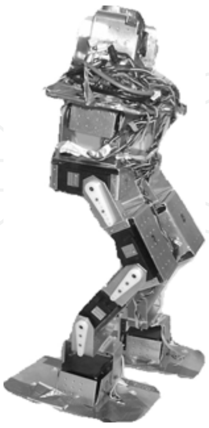

Fig. 1 The biped robot "Dany Walker"

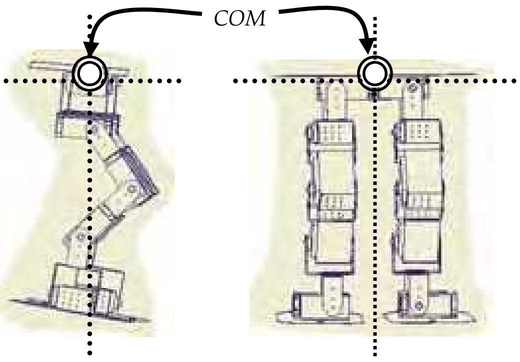

Fig. 2. Dany Walker's *COM* location.

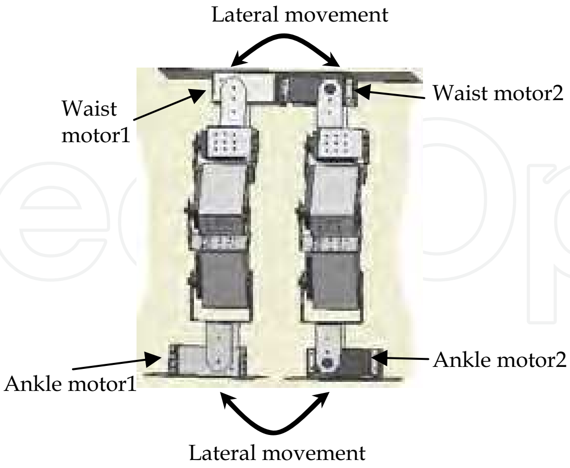

Fig. 3. Lateral balance of the motors.

3. Balance control criterion

We used the dynamic walking model to define our balance criterion. It consists of maintaining the *Zero Moment Point* (*ZMP*) inside the support region (Vukobratovic & Juricic, 1969; Vukobratovic, 1973). We implemented a feedback-force system to calculate the *ZMP*, and feed it in to the fuzzy PD incremental controller to calculate the *ZMP* error. Then, the controller adjusts the lateral robot's positions to maintain the *ZMP* point inside of the support region.

To achieve stable dynamic walking, the change between simple supports phase and double supports phase should be smooth. In the beginning of the double supports phase, the foot returns from the air and impacts against the floor, generating strong forces that affect the walking balance (Cuevas et al., 2005). The intensity of these forces is controlled by imposing velocity and acceleration conditions on saggital motion trajectories. This is achieved by using smooth cubic interpolation to describe the trajectories. In this chapter, we only discuss the control of the lateral motion (balance).

3.1 Zero Moment Point (ZMP)

The *ZMP* is the point on the ground where the sum of all momentums is zero. Using this principle, the *ZMP* is computed as follows:

$$x_{ZMP} = \frac{\sum_i m_i(\ddot{z}+g)x_i - \sum_i m_i \ddot{x} z_i - \sum_i I_{iy} \ddot{\theta}_{iy}}{\sum_i m_i(\ddot{z}+g)} \quad (1)$$

$$y_{ZMP} = \frac{\sum_i m_i(\ddot{z}+g)y_i - \sum_i m_i \ddot{x} z_i - \sum_i I_{ix} \ddot{\theta}_{ix}}{\sum_i m_i(\ddot{z}+g)}, \quad (2)$$

where ***(x_{ZMP}, y_{ZMP},0)*** are the *ZMP* coordinates, ***(x_i ,y_i ,z_i)*** is the mass center of the link *i* in the coordinate system, m_i is the mass of the link *i*, and *g* is the gravitational acceleration. I_{ix} and I_{iy} are the inertia moment components, θ_{iy} and θ_{ix} are the angular velocity around the axes *x* and *y*, taken as a point from the mass center of the link *i*. The force sensor values are directly used to calculate the *ZM*. For the lateral control, it is only necessary to know the *ZMP* value for one axis. Thus, the *ZMP* calculus is simplified using the formula

$$P_{ZMP} = \frac{\sum_{i=1}^{3} f_i \mathrm{r}_i}{\sum_{i=1}^{3} f_i}, \quad (3)$$

where f_i represents the force at the i sensor, and r_i represents the distance between the coordinate origin and the point where the sensor is located. Figure 4 shows the distribution of sensors (marked with tree circles) used for each robot's foot.

The total *ZMP* is obtained by the difference between the ZMPs at each foot:

$$Total\_P_{ZMP} = P_{ZMP1} - P_{ZMP2}, \quad (4)$$

where P_{ZMP1} is the *ZMP* for one foot and P_{ZMP2} is the ZMP for the other.

Figure 5 shows the *ZMP* point (black point) for two robot's standing cases, one before to give a step (left), and other after give a step (right). The pointed line represents the support polygon.

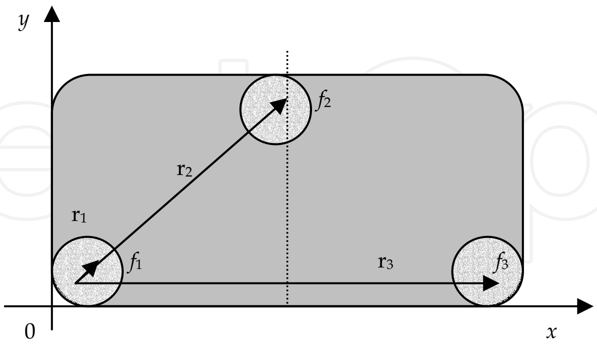

Fig. 4. Sensors distribution at the robot's foot.

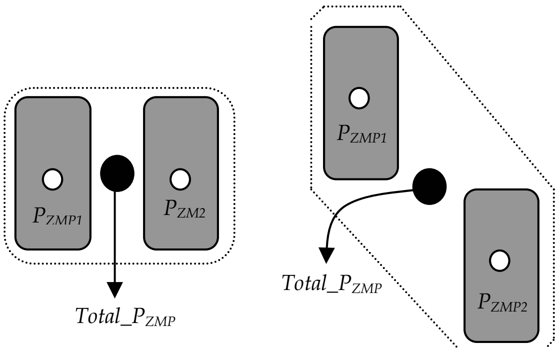

Fig. 5. The black point represents the Robot ZMP before giving a step (left), and after giving a step (right).

4. The Fuzzy PD incremental algorithm.

We propose the fuzzy PD incremental control algorithm, as a variant for the fuzzy PD controller (Sanchez et al., 1998), to implement the biped balance control. The fuzzy PD incremental control algorithm consists of only four rules and has the structure illustrated in Fig. 6.

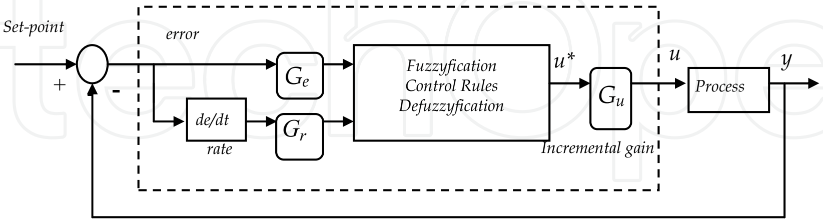

Fig. 6. Fuzzy PD incremental algorithm structure.

The gains G_u, G_e and G_r are determined by tuning and they correspond respectively to the output gains, the error (*ZMP error*) and error rate (*ZMP rate*) gains. The value u^* is the defuzzyficated output or "crisp" output. The value u is

$$u = \begin{cases} G_u * (u^*) \quad if\,|e| < \theta \quad (for \quad t = 0,\ G_{inc} = 0) \\ \\ G_{inc} + Inc \qquad if\,|e| > \theta \end{cases} \tag{5}$$

Where e is the error (error*G_e), θ is an error boundary selected by tuning, and G_{inc} is the incremental gain obtained adding the increment "*Inc*".
Figure 7 shows the flow diagram for the incremental gain of u.

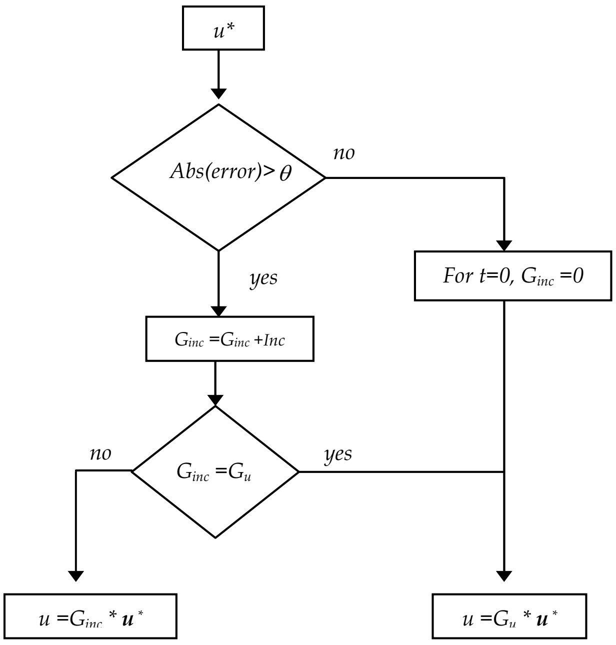

Fig. 7. Flow diagram for the incremental gain of G_u.

Figure 8 shows the area where the absolute error is evaluated and the controller output is incremental (u=G_{inc}+Inc).

4.1 Fuzzyfication

As is shown in figure 9, there are two inputs to the controller: error and rate. The error is defined as:

$$error = setpoint - y \tag{6}$$

Rate it is defined as it follows:

$$rate = (ce - pe) / sp \tag{7}$$

Where *ce* is the current error, *pe* is the previous error and *sp* is the sampling period. Current and previous error, are referred to an error without gain. The fuzzy controller has a single incremental output, which is used to control the process

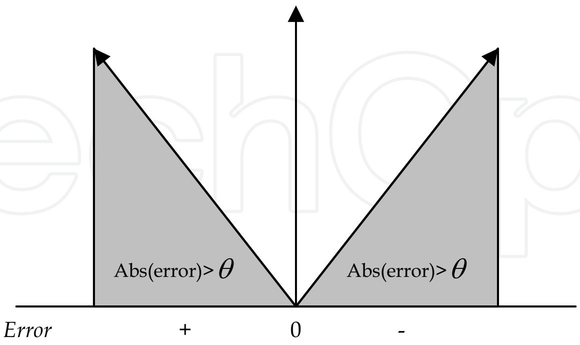

Fig. 8. Fuzzy PD incremental absolute error area.

The input an output membership functions for the fuzzy controller are shown in Fig. 9 and Fig. 10, respectively. Fig. 9 shows that each input has two linguistic terms. For the error input are: *Ge* negative error* (*en*) and *Ge* positive error* (*ep*) and for the rate input are: *Gr*negative rate* (*rn*) and *Gr * positive rate* (*rp*), while the output fuzzy terms are shown in Fig. 10 and they are: *Negative output* (*on*), *Zero output* (*oz*) and *Positive output* (*op*).

As shown in Fig. 9, the same function is applied for *error* and *rate* but with different scaling factors: *Ge* and *Gr* respectively.

H and L are two positive constants to be determined. For convenience we will take H=L to reduce the number of control parameters to be determined. The membership functions for the input variables, error and rate, are defined by:

$$\begin{aligned} \mu_{ep} &= \frac{L+(G_e * error)}{2L} \\ \mu_{en} &= \frac{L-(G_e * error)}{2L} \\ \mu_{rp} &= \frac{L+(Gr * rate)}{2L} \\ \mu_{rn} &= \frac{L-(Gr * rate)}{2L} \end{aligned} \tag{8}$$

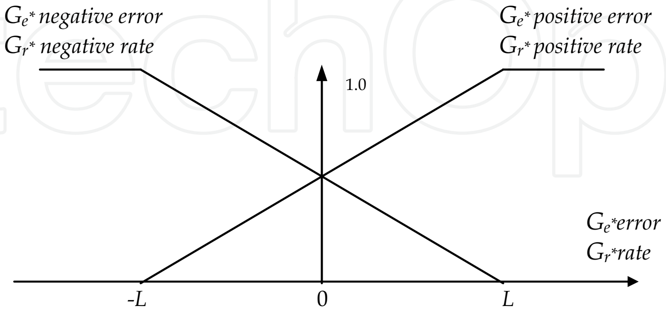

Fig. 9. Input membership functions.

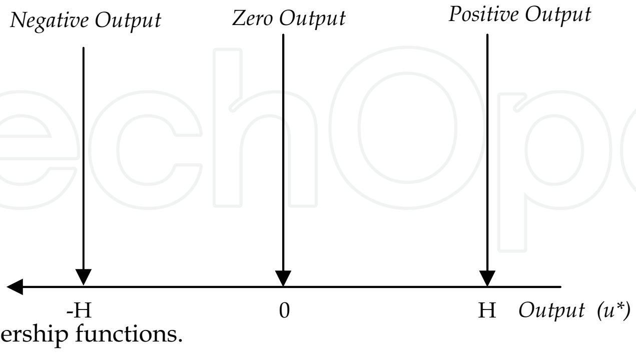

Fig. 10. Input membership functions.

4.2 Fuzzy rules and defuzzyfication.

There exist four rules to evaluate the fuzzy PD incremental controller (Miller 1994):

R1. If *error* is *ep* and *rate* is *rp* then output is *op*

R2. If *error* is *ep* and *rate* is *rn* then output is *oz*

R3. If *error* is *en* and *rate* is *rp* then output is *oz*

R4. If *error* is *en* and *rate* is *rn* then output is *on*

The determination of these rules can be accomplished easily if the system evolution is analyzed in the different operation points. For example, when the *error* and the *rate* increase (rule 1), it means that the system response decreases and moves away from the *setpoint*, for this reason it is necessary to apply a *positive* stimulus that allows to increase the system output. The figure 11 shows the determination of the different rules based on the system response.

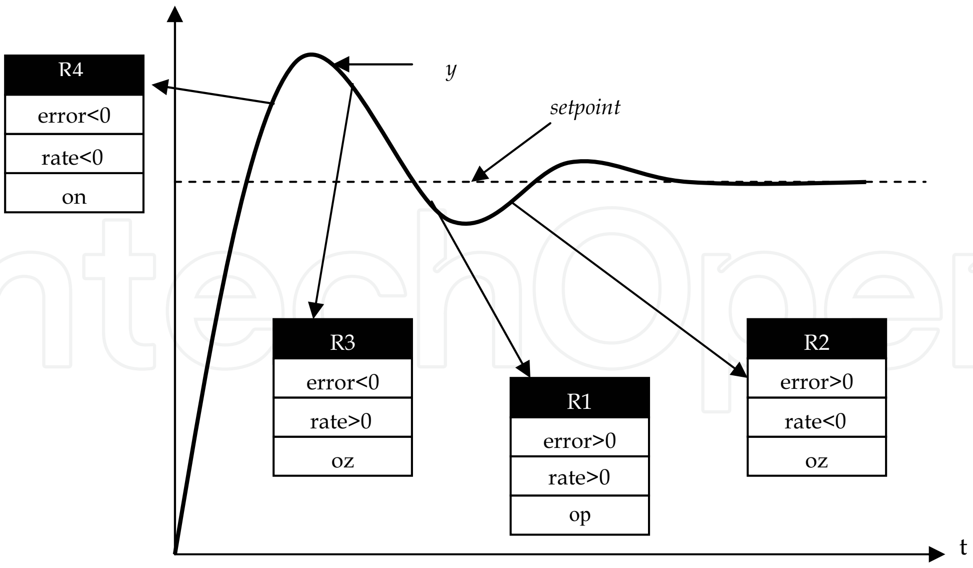

Fig. 11. Determination of the different rules based on the system response (see Text).

For the fuzzy condensed controller proposed, the input error and rate values ranges can be represented in 20 input regions (IC), like is shown in Fig. 12. If the membership functions are evaluated, the 4 control rules, the simplification H=L, and the defuzzyfication is applied in each one of the 20 inputs combinations, then 9 equations can be obtained (Sanchez et al., 1998), which can determine the control signal u that should be applied, depending on the region it is located. In other words, to implement the fuzzy condensed controller, only will be necessary to know the region in which the inputs variables are located and later evaluate the corresponding equation for this region. For example, the first equation acts in regions IC1, IC2, IC5, IC6. The figure 13 shows the control surface of the fuzzy condensed controller considering H=L=1.

Finally, the defuzzyfication method used is the gravity center, in this case is represented by:

$$u = \frac{-H(\mu_{R4(x)}) + 0(\mu_{R2(x)+}\mu_{R3(x)}) + H(\mu_{R1(x)})}{\mu_{R4(x)} + (\mu_{R2(x)+}\mu_{R3(x)}) + \mu_{R1(x)}} \tag{9}$$

5. Real time results

The first test applied to the balance controller was an x-direction impulse. The robot was standing in balance and then a push in the lateral direction was applied to the biped robot. Figure 14 shows the evolution of the *ZMP* value in centimeters during 10 seconds.

Figure 15 shows the error and rate evolution during the application of the x-direction impulse. The incremental PD fuzzy controller's parameters were: *Ge*=2, *Gr*=2, and *Gu*=1.

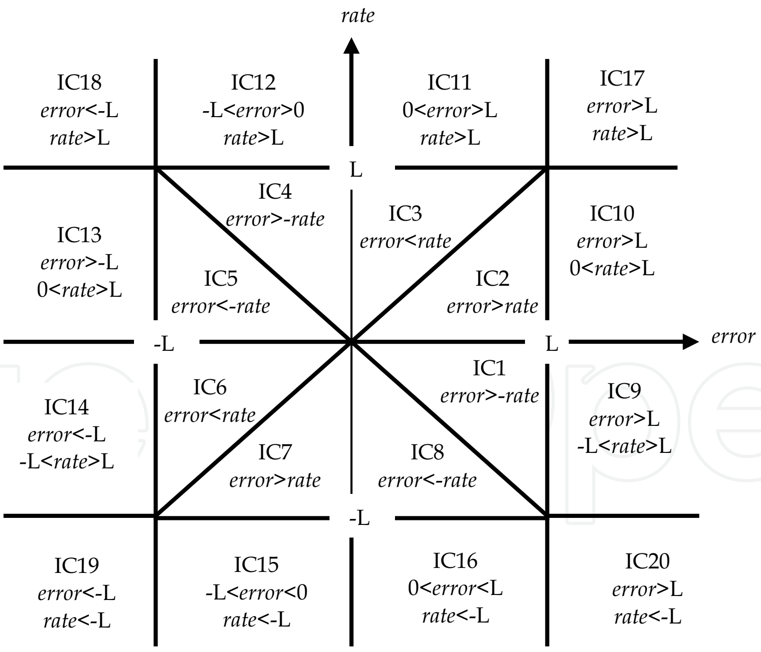

Fig. 12. Input regions.

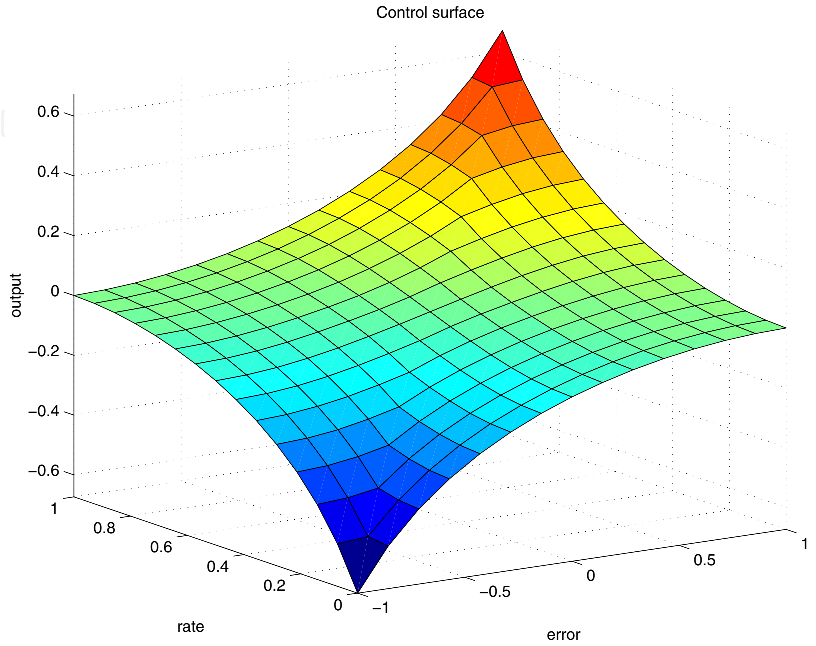

Fig. 13. Control surface of the fuzzy condensed controller considering H=L=1.

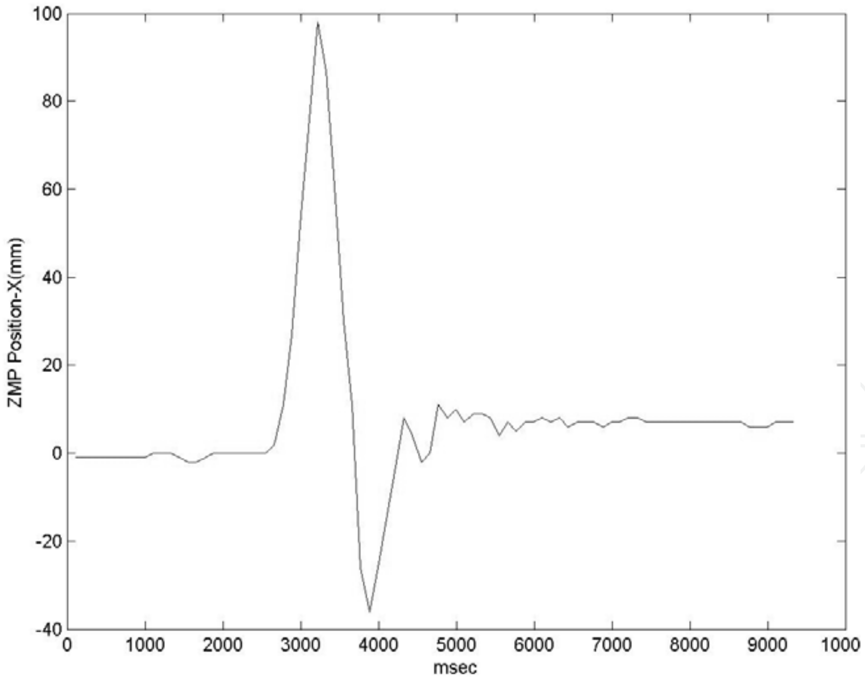

Fig. 14. ZMP value evolution achieved by the controller, for a x-direction impulse.

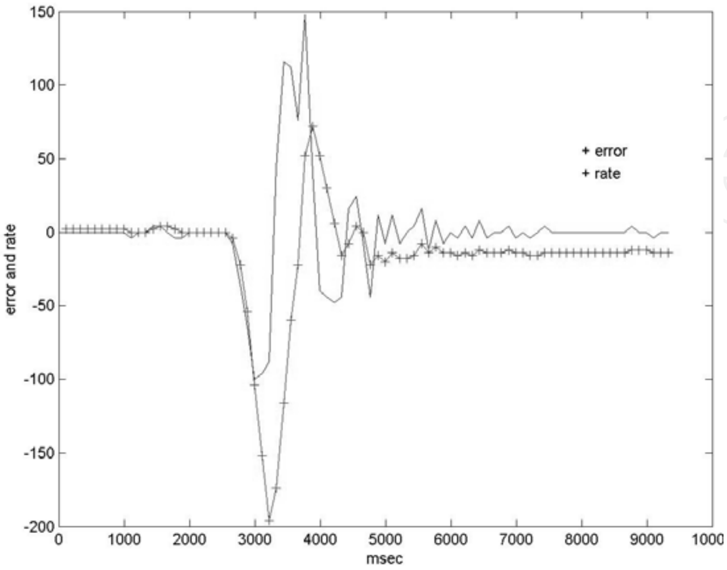

Fig. 15. Error and rate evolution for a *x*-direction impulse.

Finally, a walking test balance was applied to the robot. The robot gave some steps in a flat surface, while the balance controller compensated the ZMP value. Figure 16 shows the evolution of the ZMP value (in centimeters) achieved by the controller during 15 seconds. Figure 17 shows error and rate evolution during the robots walk. The incremental PD fuzzy controller's parameters were: *Ge*=2, *Gr*=2, and *Gu* =1.

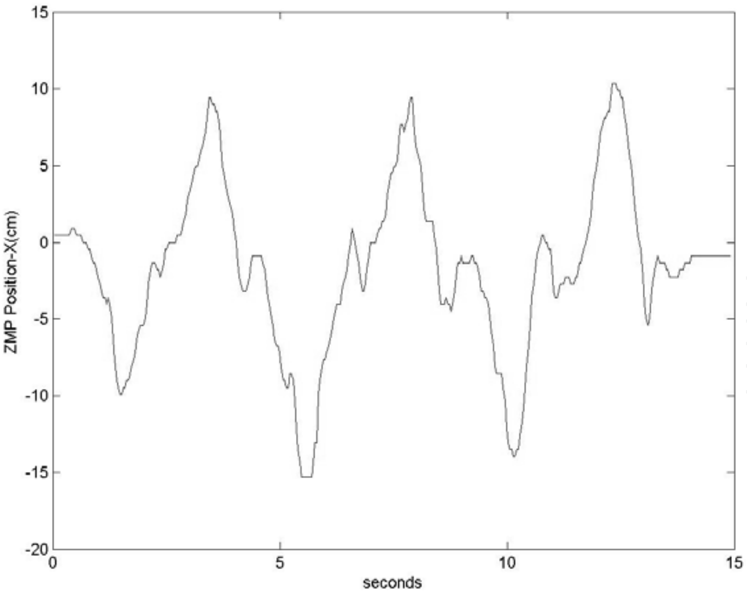

Fig. 16. ZMP value evolution achieved by the controller during the robot walk.

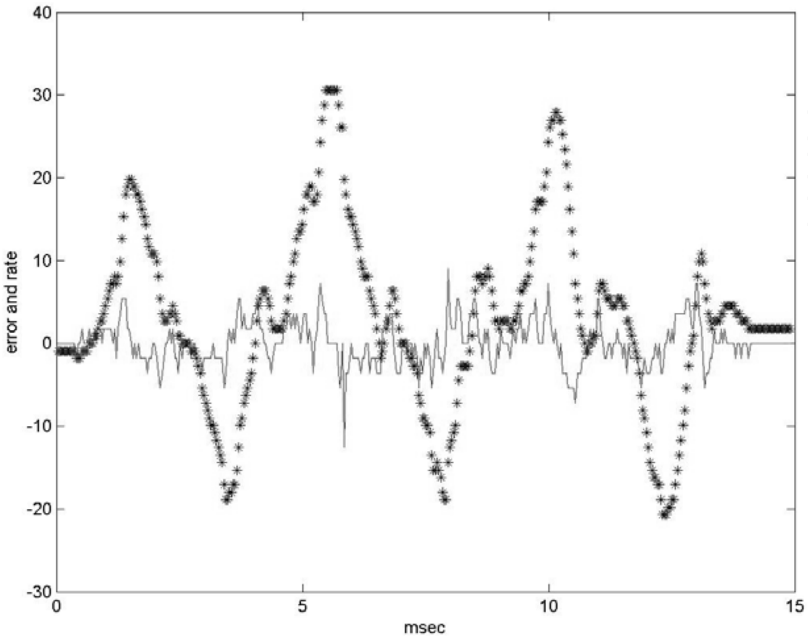

Fig. 17. Error and rate evolution during the robot walk.

The motor's position output was computed by the controller during the walk. It is showed at Figure 18. This motor's position value is only just for one waist motor.

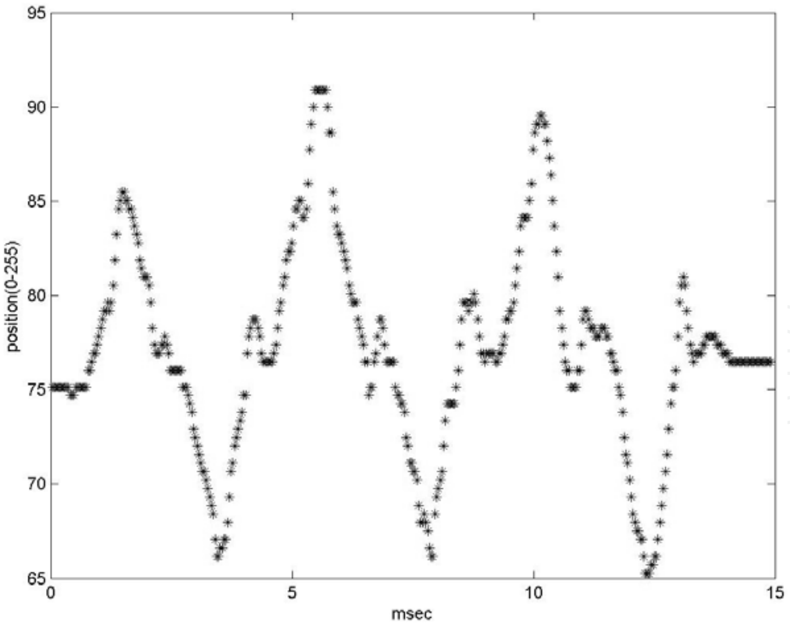

Fig. 18. Motor's position output during the robot walk..

6. Conclusion

Figure 11 shows the controller's performance and response for an *x*-direction impulse. The response was fast, approximately 2 seconds, until the controller reached a *ZMP* value near to zero. This feature allows the biped robot to gain stability even during walking (figure 13), maintaining the *ZMP* always inside the support polygon.

Our experiments with the fuzzy PD incremental controller algorithm demonstrated that it is computationally economic, all running in a PIC microcontroller, and appropriated for balance control. The algorithm was successfully used in real-time with the biped robot "Dany walker" (videos available at http://www.inf.fu-berlin.de/~zaldivar).

The algorithm proposed in this chapter could be also used in other robots structures with a different dynamic, and even with other degrees of freedom. It would be only necessary to adjust the controller's gain parameters to the particular structure.

We plan to use the information given by an inclinometer along with the *ZMP* value. In this case, the goal of the bipedal balance robot control will be to achieve an inclination value of cero and to maintain the *ZMP* at the center, or inside of the support polygon.

The bipedal robot used in this work is part of a project that is being developed at the Freie Universität Berlin.

7. References

Goddard, R.; Zheng, Y. & Hemami, H. (1992). Control of the heel-off to toe-off motion of a dynamic biped gait, *IEEE Trans. Syst. Man. Cayb.,* 1992, *vol.22*, no. 1

Kanehira, N.; Kawasaki, T.; Ohta, S.; Isozumi, T.; Kawada, T.; Kanehiro, F.; Kajita, S. & Kaneko, K. (2002). Design and experiments of advanced module (HRPL-2L) for humanoid robot (HRP-2) development, Proc. 2002, IEEE-RSJ *Int. Conf. Intell. Rob. Sys. EPFL*, Lausanne, Switzerland, 2002, 2455-2460.

Konno, A.; Kato, N.; Shirata, S.; Furuta, T. & Uchiyama, M. (2000). Development of a light-weight biped humanoid robot in Proc. 2000 *IEEE-RSJ Int. Con. Intell. Rob. Sys.*, 2000, 1565-1570.

Miller, W. (1994). Real-time neural network control of a biped walking robot*, IEEE contr. Syst., vol. 14,* 1994, 41-48.

Yamaguchi, J.; Soga, E.; Inoue, S. & Takanishi, A. (1999). Development of a biped robot-control method of a whole body cooperative dynamic biped walking, in Proc. 1999 *IEEE Int. Conf. Robot. And Aut.,* Detroit, Michigan, 1999, 368-374.

Taga, G.; Yamaguchi Y. & Shimizu, H. (1991). Self-organized control of bipedal locomotion by neural oscilators in unpredictable environment, *Biol. Cyb. 65* 1991, 147-165.

Kajita, S.; Yamaura, T. & Kobayashi, A. (1992). Dynamic walking control of a biped robot along a potiential energy conserving orbit, *IEEE Trans. Robot Automat. Vol. 8*, no. 4, 1992. pp 437-438.

Zheng, Y. & Shen, J. (1990). Gait synthesis for the SD-2 biped robot to climb sloped surface, *IEEE, Trans. Robot Automat. Vol 6*, no 1. , 1990, 86-96.

Cuevas, E.; Zaldívar, D. & Rojas, R. (2004). Bipedal robot description, *Technical Report B-03-19, Freie Universität Berlin, Fachbereich Mathematik und Informatik*, Berlin, Germany, 2004.

Vukobratovic, M. & Juricic, D. (1969). Contribution to the synthesis of biped gait, *IEEE Trans. Bio-Med. Eng., vol. BME-16,* no. 1 , 1969, 1-6.

Vukobratovic, M. (1973). How to control artificial anthropomorphic system, *IEEE Trans. Syst. Man. Cyb., vol. SMC-3,* no. 5, 1973, 497-507.

Cuevas, E.; Zaldívar, D. & Rojas, R. (2005). Dynamic Control Algorithm for a Biped Robot, *The 7th IASTED International Conference on CONTROL AND APPLICATIONS,Cancún, México, CA 2005.*

Sanchez, E.; Nuno, L.; Hsu, Y. & Guanrong, C. (1998). Real Time Fuzzy Swing-up Control for an Underactuated Robot, *JCIS '98 Proceedings,Vol 1* , N.C., USA, 1998.

Humanoid Robots: New Developments

Edited by Armando Carlos de Pina Filho

ISBN 978-3-902613-00-4
Hard cover, 582 pages
Publisher I-Tech Education and Publishing
Published online 01, June, 2007
Published in print edition June, 2007

For many years, the human being has been trying, in all ways, to recreate the complex mechanisms that form the human body. Such task is extremely complicated and the results are not totally satisfactory. However, with increasing technological advances based on theoretical and experimental researches, man gets, in a way, to copy or to imitate some systems of the human body. These researches not only intended to create humanoid robots, great part of them constituting autonomous systems, but also, in some way, to offer a higher knowledge of the systems that form the human body, objectifying possible applications in the technology of rehabilitation of human beings, gathering in a whole studies related not only to Robotics, but also to Biomechanics, Biomimmetics, Cybernetics, among other areas. This book presents a series of researches inspired by this ideal, carried through by various researchers worldwide, looking for to analyze and to discuss diverse subjects related to humanoid robots. The presented contributions explore aspects about robotic hands, learning, language, vision and locomotion.

InTech Europe
University Campus STeP Ri
Slavka Krautzeka 83/A
51000 Rijeka, Croatia
Phone: +385 (51) 770 447
Fax: +385 (51) 686 166
www.intechopen.com

InTech China
Unit 405, Office Block, Hotel Equatorial Shanghai
No.65, Yan An Road (West), Shanghai, 200040, China
中国上海市延安西路65号上海国际贵都大饭店办公楼405单元
Phone: +86-21-62489820
Fax: +86-21-62489821